Impact of I/Q Imbalance on Time Reversal-based Indoor Positioning Systems

Trung-Hien Nguyen[1], Jérôme Louveaux[2], Philippe De Doncker[1], and François Horlin[1]
[1]OPERA department, Université libre de Bruxelles (ULB), 1050 Brussels, Belgium
[2]ICTEAM institute, Université catholique de Louvain (UCL), 1348 Louvain-la-Neuve, Belgium
Email: trung-hien.nguyen@ulb.ac.be

***Abstract*—Time reversal has been shown as a promising technology for the indoor positioning. Instead of mitigating the multipath channel, the time reversal based indoor positioning system (TRIPS) exploits the rich multipath propagation in indoor environments as a specific signature for each location. In order to do this, a database should be first constructed by channel probing. The devices used in this process are assumed to have no hardware impairments or be well calibrated. However, the low cost terminal to be located can exhibit impairments, such as I/Q imbalance at the front end transmitter known to create an interference image of the signal that can particularly impact the performance of time reversal. In this paper, we investigate the impact of the I/Q imbalance on the TRIPS. We analytically show that the I/Q imbalance modifies the metric used for the localization and hence reduces the spatial focusing gain of TRIPS. Numerical simulations are carried out to evaluate this observation. The results further show that the I/Q imbalance creates errors in the positioning estimation. More specifically, at the gain and phase imbalances of respectively 1.1 and 10°, the focusing gain reduction is about 0.5 dB while the estimation error rate is increased by about 5% in the specified scenario.**

***Index terms*—** Indoor positioning system, time reversal, I/Q imbalance, OFDM.

I. Introduction

The Global Positioning System (GPS) has been successful to achieve a good accuracy of the order of meters for outdoor localization. However, the GPS generally fail to localize the objects in the indoor environments because the GPS signals become too weak after propagation through the concrete walls. With the increase in demands of location-based information services like tourist guidance in a museum, advertisement in the smart market, etc., a high accuracy indoor positioning system (IPS) needs to be developed. A lot of researchers investigate the use of the current local area network (LAN) infrastructure integrated with the indoor positioning techniques in order to obtain a good IPS.

Among indoor positioning technologies, the fingerprinting method has become an attractive technology. Early works proposed to build the fingerprints are based on the received signal strength (RSS) [1]. However, the estimation accuracy is limited to several meters. Furthermore, in the strong non-line-of-sight (NLOS) condition, the positioning estimation based on the RSS becomes troublesome. By using channel impulse response (CIR) estimated during the communications, a finer grained information for localization can be obtained that improves the accuracy to the order of tens of centimeters, for example the FIFS [2]. To further exploit the existing Wi-Fi systems which are based on orthogonal frequency division multiplexing (OFDM) technique, i.e., 802.11n/ac, the channel frequency response (CFR) is also used as the fingerprints for IPS. Recently, an innovative IPS based on the time reversal technique has been proposed in [3], in which the accuracy was reported down to 10 cm within a 0.9×1 m area-of-interest making it a promising technology for the IPS.

Time reversal based indoor positioning system (TRIPS) operates based on two phases: (i) offline CIR (or CFR) estimation probing phase to build the database and (ii) localization estimation based on the correlation between the online estimated CIR (or CFR) and the ones in the database. Usually, the access point (AP) stores the CIR database for the localization in order to reduce the cost of the user terminal (UT). While the reference terminal can generally assume to not be prone to hardware impairments, it is not the case for the UT to be located. One of the major source of impairments in wireless systems is the imbalance between the in-phase (I) and the quadrature (Q) branches, referred to as I/Q imbalance, where the up-down complex frequency conversion by the sinusoidal oscillators happens. Typically the I/Q imbalance originates from the mismatch between the I and Q branches compared to the ideal case, in which the phase difference is 90° and the amplitudes are equal to each other. The I/Q imbalance and its influence on the wireless systems have been well-documented in the literature, i.e., [4], [5] and references therein. However, the impact of I/Q imbalance on the TRIPS has not been studied so far.

In this paper, we study for the first time the impact of I/Q imbalance on the TRIPS. We investigate the impact of I/Q imbalance on the localization metric proposed for TRIPS [6], and on the spatial focusing effect as well as on the failure ratio of the positioning estimation.

Symbolic notation: the underlined low-case and upper-case letters present the column vectors of the time-

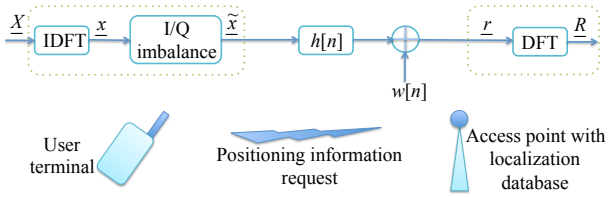

Fig. 1. A time reversal based positioning system with I/Q imbalance at the transmitter.

domain and frequency-domain variables, respectively, the double-underlined upper-case letter presents a matrix, $\underline{\underline{I}}_M$ is the $M \times M$ identity matrix and $\underline{\underline{J}}_M$ is the $M \times M$ anti-diagonal identity matrix, i.e. the first row of $\underline{\underline{I}}_M$ is the M-th row of $\underline{\underline{J}}_M$, the second row of $\underline{\underline{I}}_M$ is the $(M-1)$-th row of $\underline{\underline{J}}_M$ and so on, $\underline{\underline{\Lambda}}_X$ is the diagonal matrix whose diagonal entry is the element of the vector $\underline{X}$, $\|\cdot\|_2$ is the Euclidean norm, $(\cdot)^*$ is the complex conjugate operator, $(\cdot)^H$ is the Hermitian transpose, $(\cdot)^T$ is the transpose operator, $\odot$ is the Hadamard product, $\otimes$ is the convolution operator, $\overline{x}$ is the mean value of vector $\underline{x}$, i.e. $\overline{x} = 1/M \sum_{m=0}^{M-1} x_m$, $\angle(\cdot)$ is the angle operator, $unwrap(\cdot)$ is the phase unwrapping operator, $\Re$ is the real part operator.

II. I/Q Imbalance and its Impact on Positioning Systems

The scenario is presented in Fig. 1, where the UT sends a request to the AP to identify its location. As the Wi-Fi technology based on OFDM modulation is used widely in the indoor environment, we propose to use an OFDM-like sequence to estimate the CFR. To do so, a frequency-domain pilot symbol $\underline{X}$ is used to form a repetitive time-domain OFDM probing frame $\underline{x}$ by using inverse discrete Fourier transform (IDFT) before being sent to the AP. The frequency-domain sequence $\underline{X}$ in the channel probing phase is constructed by a known uniformly distributed sequence composed of $\{\pm 1\}$. However the UT front-end can suffer from I/Q imbalance leading to the modified transmitted signal $\underline{\tilde{x}}$ as follows

$$\underline{\tilde{x}} = \mu \cdot \underline{x} + \nu \cdot \underline{x}^*, \tag{1}$$

in which μ and ν are the coefficients dependent on the gain imbalance ϵ and the phase imbalance θ [4]

$$\begin{aligned} \mu &= \cos\theta + j \cdot \epsilon \sin\theta \\ \nu &= \epsilon \cos\theta + j \cdot \sin\theta \end{aligned}. \tag{2}$$

After propagation through the channel and addition of a white Gaussian noise (AWGN), the frequency-domain received signal can equivalently be written as

$$\underline{R} = \left(\mu \cdot \underline{X} + \nu \cdot \underline{\underline{J}} \cdot \underline{X}^*\right) \odot \underline{H} + \underline{W}, \tag{3}$$

where $\underline{H}$ and $\underline{W}$ are the frequency-domain vectors of the channel and noise, respectively. Assuming that $\underline{X}$ is known at the receiver and define $\underline{Y} = \underline{\underline{J}} \cdot \underline{X}^*$, the estimated CFR is given by

$$\begin{aligned} \widehat{\underline{G}} &= \underline{\underline{\Lambda}}_X^{-1} \cdot (\mu \cdot \underline{X} + \nu \cdot \underline{Y}) \odot \underline{H} + \underline{\underline{\Lambda}}_X^{-1} \cdot \underline{W} \\ &= \left(\mu \cdot \underline{\underline{I}} + \nu \cdot \underline{\underline{\Lambda}}_X^{-1} \cdot \underline{\underline{\Lambda}}_Y\right) \cdot \underline{H} + \underline{\underline{\Lambda}}_X^{-1} \cdot \underline{W} \end{aligned}. \tag{4}$$

Without I/Q imbalance, i.e. $\mu = 1$ and $\nu = 0$, the estimated CFR logically reduces to

$$\widehat{\underline{H}} = \underline{\underline{\Lambda}}_X^{-1} \cdot \underline{R} = \underline{H} + \underline{\underline{\Lambda}}_X^{-1} \cdot \underline{W}. \tag{5}$$

Without compensation for the I/Q imbalance, the estimated CFR is modified by an independent term that depends on the pilot sequence and on the image of the CFR and its consequence in the time reversal based indoor positioning systems (TRIPS) is studied in the next Section.

III. Time Reversal based Indoor Positioning System

We study the indoor localization problem where there is an AP and an UT in an indoor environment. The AP is positioned in an arbitrarily known location, whereas the location of the UT needs to be identified. In the TRIPS system, a database mapping the physical geographical locations to the logical locations in the CFR space is firstly built offline. Then, the online estimated CFR of the UT is compared to the CFRs in the database and the one with the highest cross-correlation gives the position of the UT. Note that, the size of the fingerprinting database is relatively small compared to the capability of the current storage devices. For instance, it is shown that we only need about 4.2 MBytes to store the database for a room of size 5.4×3.1 m [3]. A better positioning resolution can be achieved by integrating the TRIPS with the machine learning approaches used in [7], however, it is beyond the scope of this paper.

A. Channel Probing and Localization Metric

We assume that the channel probing sequence is known at the receiver. Since the CFR can efficiently be estimated based on (5) using the well-defined preamble sequence, we use here the frequency domain expression of the TR resonating strength in [3] as the localization metric to estimate the positioning of UT and it is defined as follows [6]

$$\Xi_m = \arg\max_{\Delta\phi,\phi_0} \left| \frac{\underline{H}_m^H \cdot \left(\widehat{\underline{H}} \odot \underline{\Omega}\left(\Delta\phi\right) \odot e^{-j\phi_0}\right)}{\|\underline{H}_m\|_2 \left\|\widehat{\underline{H}}\right\|_2} \right|^2, \tag{6}$$

where $\underline{H}_m$ denotes the CFR at the logical position m in the database, $\underline{\Omega}\left(\Delta\phi\right)$ is the rotation vector whose

element is $\Omega_k = \exp(-j2\pi \cdot k \cdot \Delta\phi)$. The calculation of $\Delta\phi$ and ϕ_0 are discussed in the next paragraph in detail. The logical position $\hat{m}$ corresponding to $\hat{m} = \arg\max_m \Xi_m$ is then transformed to the geographical information in order to identify the location of the UT.

Note that, whenever the receiver realizes a channel probing request for the localization, it starts estimating the CFR that incorporates a possible channel time delay. We hence introduce the phase rotating vector $\underline{\Omega}(\Delta\phi)$ in (6) to represent the timing offset compensation coming from the fact that the preamble frame is not time synchronized. The timing offset in the time domain will create a linear slope of phase in the frequency domain. Instead of using two-dimensional searching for the problem in (6), we use here a linear least square fitting solution to find the angle of this slope as follows

$$\varphi = \tan^{-1}\left(\frac{\sum_{m=0}^{M-1}\kappa_m \cdot \Theta_m - M \cdot \overline{\kappa} \cdot \overline{\Theta}}{\sum_{m=0}^{M-1}\kappa_m^2 - M \cdot (\overline{\kappa})^2}\right), \quad (7)$$

in which $\underline{\Theta}$ is the vector stacking the phase unwrapping values of the CFR vector, i.e. $\underline{\Theta} = unwrap\left(\angle\underline{\widehat{H}}\right)$ and $\underline{\kappa} = [0\ 1\ 2\ ...\ M-1]^T$, M is the number of the subcarriers. The slope is compensated in the CFR of the database and in the online estimated CFR.

B. Localization Metric under the I/Q Imbalance Impact

It can be seen that in (6), Ξ_m takes values in the range $[0, 1]$. When the CFR between the AP and the UT matches the one represented to the position m in the database, Ξ_m is close to 1. However, as aforementioned the estimated CFR under the impact of I/Q imbalance is modified, resulting in a change of the localization metric Ξ_m. Assuming that the phase rotating vector in (6) is correctly calculated and that the considered position of the UT associated with the CFR $\underline{\widehat{G}}$ is matched with the desired position of the CFR $\underline{H}_m$ in the database, from (4), (6) and removing the index for simplicity, the corresponding localization metric is presented as follows

$$\Xi = \left|\frac{\underline{H}^H \cdot \underline{\widehat{G}}}{\|\underline{H}\|_2 \cdot \left\|\underline{\widehat{G}}\right\|_2}\right|^2. \quad (8)$$

We define the vector $\underline{\Psi}$ as follows

$$\underline{\Psi} = \nu \cdot \underline{\underline{\Lambda}}_X^{-1} \cdot \underline{\underline{\Lambda}}_Y \cdot \underline{H} + (1-\mu) \cdot \underline{\underline{\Lambda}}_X^{-1} \cdot \underline{W}. \quad (9)$$

The estimated CFR can be re-written as $\underline{\widehat{G}} = \mu \cdot \underline{H} + \underline{\Psi}$ and the localization metric in (8) can be represented by

$$\Xi = \frac{\left|\underline{H}^H \cdot (\mu \cdot \underline{H} + \underline{\Psi})\right|^2}{\left(\|\underline{H}\|_2 \cdot \|\mu \cdot \underline{H} + \underline{\Psi}\|_2\right)^2}. \quad (10)$$

After some manipulation, we can get the expression of the localization metric as in (11). Based on the Cauchy-Schwarz inequality [9], the following relation holds

$$\left|\sum_{k=0}^{M-1} H_k \cdot \Psi_k\right|^2 \leq \sum_{k=0}^{M-1}|H_k|^2 \cdot \sum_{k=0}^{M-1}|\Psi_k|^2 = \left(\|\underline{H}\|_2\right)^2 \cdot \left(\|\underline{\Psi}\|_2\right)^2. \quad (12)$$

As a consequence, it is demonstrated that the localization metric decreases under the impact of I/Q imbalance for the correct position, i.e., $\Xi \leq 1$, even if the estimated CFR between the AP and the UT matches the one in the database. The equality happens when the vectors $\underline{H}$ and $\underline{\Psi}$ are linearly dependent. It can however be observed from (5) and (9) that these two vectors are independent from each other in the presence of the I/Q imbalance. It implies that $\Xi < 1$ or in another words, the focusing gain of TRIPS is reduced in the presence of the I/Q imbalance. The reduction of the focusing gain is numerically studied in the next Section.

IV. Numerical Study

An indoor room of size $5 \times 5 \times 3$ m is considered. In order to study the impact of I/Q imbalance on TRIPS, the deterministic indoor channel model is simulated by using a ray tracing software and the focusing gain reduction and the estimation failure ratio are assessed. We fix the bandwidth $B = 400$ MHz for all the simulations. The OFDM symbol length (or the DFT size) is fixed to 512. For each value of the signal-to-noise ratio (SNR), 1000 noise realizations are carried out to calculate the average value and its standard deviation (if necessary).

A. Channel Model

The ray tracing technique is used to simulate the multipath-component channel [8]. In order to save time, we limited our simulations to the third-order reflection and the diffuse scattering was ignored. In the simulation, we use 3-D model with bounded planes in combination with the image method to compute the rays. Both line-of-sight (LOS) and non-line-of-sight (NLOS) are considered. In the NLOS case, the direct path representing for the LOS is removed, which could physically represent a situation where an obstacle hides the transmitter to the receiver. The CIR assumed to be temporally static can be modeled as follows

$$h(\tau) = \sum_{l=1}^{L} \alpha_l e^{-j(2\pi f_c \tau_l + \xi)} \delta(\tau - \tau_l), \quad (13)$$

where L is the total number of multipath components including the LOS path when it exists, α_l is the attenuation linked to the path loss and the reflection associated with that multipath component. In this model, we assume that the phase change comes from the delay τ_l being $2\pi f_c \tau_l$

$$\Xi = \frac{\left|\mu^2\right| \cdot \left(\|\underline{H}\|_2\right)^4 + \left|\sum_{k=0}^{M-1} H_k \cdot \Psi_k\right|^2 + 2\left(\|\underline{H}\|_2\right)^2 \sum_{k=0}^{M-1} \Re\left\{\mu \cdot H_k \cdot \Psi_k\right\}}{\left|\mu^2\right| \cdot \left(\|\underline{H}\|_2\right)^4 + \left(\|\underline{H}\|_2\right)^2 \cdot \left(\|\underline{\Psi}\|_2\right)^2 + 2\left(\|\underline{H}\|_2\right)^2 \sum_{k=0}^{M-1} \Re\left\{\mu \cdot H_k \cdot \Psi_k\right\}}. \tag{11}$$

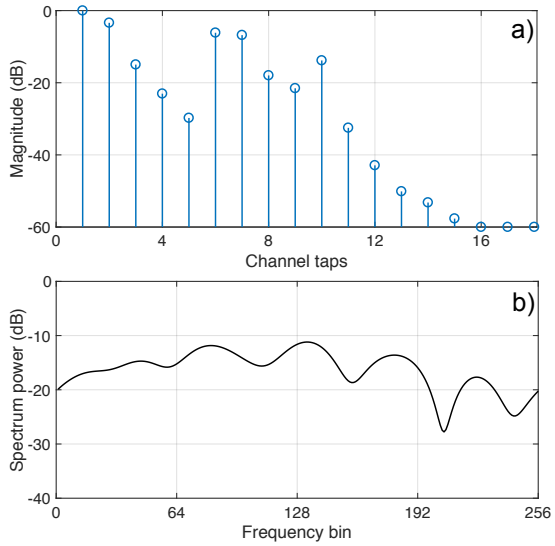

Fig. 2. Examples of (a) ray-tracing based channel impulse response simulation and (b) its associated frequency-domain output.

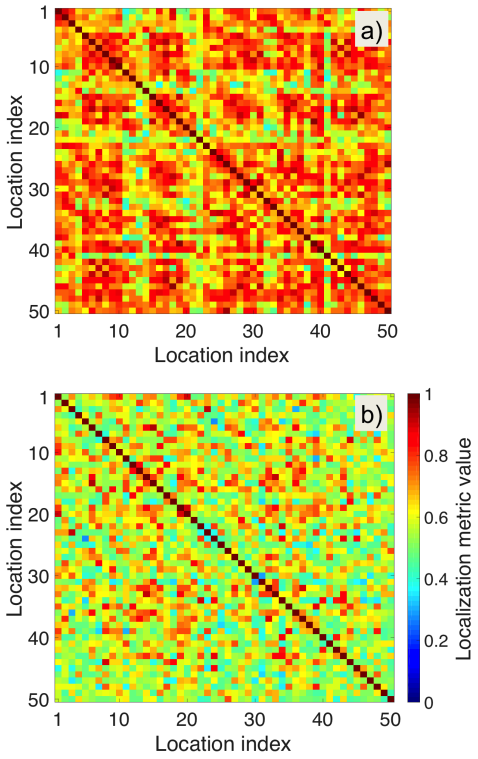

Fig. 3. Localization metric values of all grid points by moving the intended location within the grid-of-interest in the (a) LOS and (b) NLOS case. Each value of (*m, n*) grid point represents the focusing gain calculated by the localization metric at location *m* when the intended location is *n*.

and deterministic phase change ξ after the reflection, where f_c is the carrier frequency. Fig. 2 shows an example of ray-tracing result from the transmitter located at $(1, 1, 1)$ m to the receiver located at $(3.1, 3.2, 1)$ m, with the bandwidth limited to 400 MHz. The number of taps of the simulated CIR is about fifteen and the CIR is normalized to the strongest channel tap (Fig. 2(a)).

B. Metrics to Evaluate the I/Q Imbalance Impact

In order to characterize the impact of I/Q imbalance to the metric of TRIPS, we define a focusing gain reduction (FGR) as the ratio between the localization metrics without (Ξ_{wo}) and with (Ξ_w) I/Q imbalance

$$FGR = 10 \cdot \log_{10}\left(\frac{\Xi_{wo}}{\Xi_w}\right). \tag{14}$$

We also characterize the correctness of the positioning estimation under the impacts of both I/Q imbalance and AWGN by calculating the ratio between the number of position estimation failures and the total number of position estimations.

V. Results

In the first step, we evaluate the localization metric in (6) in the absence of the I/Q imbalance. Fig. 3 shows the localization metric values of 50 position points within the area of interest. The distance between two points in the grid is equal to the carrier wavelength, i.e. 12.5 cm. Each point is consecutively considered as an intended location, by moving the intended location within the grid of interest we get the focusing gains for each intended point in the LOS (Fig. 3(a)) and NLOS (Fig. 3(b)) cases. It can be observed that the NLOS case provides a better focusing gain compared to the LOS case, thanks to the more uniqueness of the CFR information. As the localization in the NLOS indoor environment is in general more challenging, in what follows we focus only on the database-aided localization in the NLOS case.

In the next step, the gain and phase imbalances are set to be 1.1 and 10°, respectively. We consider a grid-of-interest with the dimension of $(100 \times 100)\lambda$, where λ is the carrier wavelength. The UT is located randomly in one point of this grid. We calculate the spatial focusing of the localization metric by substituting the estimated CFR between the AP and UT and each CFR in the

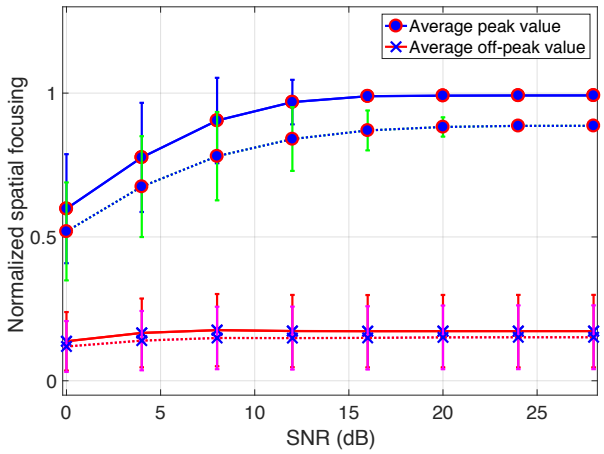

Fig. 4. Average peak values, average off-peak values of localization metrics and its associated standard deviation as the function of SNRs without (solid lines) and with (dashed lines) I/Q imbalance of $\epsilon = 1.1$ and $\phi = 10^\circ$.

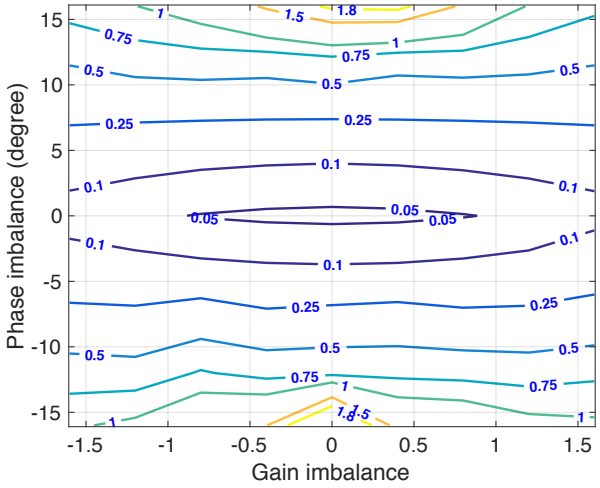

Fig. 6. Focusing gain reduction contour for different gain and phase imbalance values at SNR = 24 dB.

database into (6).

Fig. 4 presents the average peak and off-peak values with different received SNR values without (solid lines) and with (dashed lines) I/Q imbalance. The standard deviation is also plotted for each SNR value. It can be seen that under the impact of I/Q imbalance the spatial focusing of the peak value is reduced about 0.5 dB (based on (14)) regardless of the SNR value, while the difference of off-peak values with and without I/Q imbalance is small. It should be reminded that the peak appears when the estimated CFR matches a CFR in the database. The off-peaks exhibit low values due to the high un-correlation between the CFRs associated with different positions.

The reduction of the spatial focusing shown in Fig. 4 implies that we may encounter more errors in the positioning estimation in the presence of the I/Q imbalance.

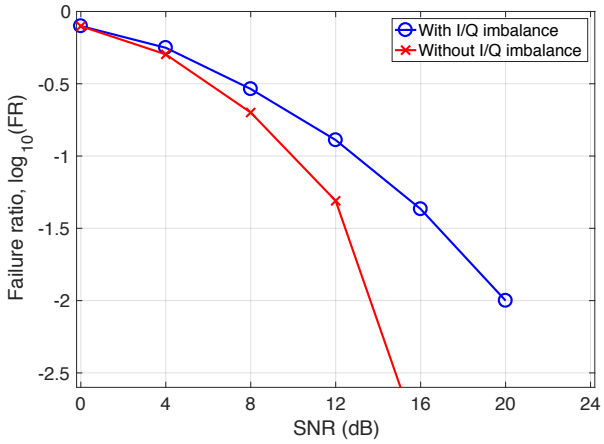

Fig. 5. Failure ratio of the positioning estimation under the impact of I/Q imbalance of $\epsilon = 1.1$ and $\phi = 10^\circ$.

To verify this hypothesis, we calculate the position estimation failure ratio. This ratio is presented in Fig. 5 both with and without I/Q imbalance. It can be observed that at very low SNR the AWGN is more dominant compared to the impact of I/Q imbalance, the failure rate (FR) is not very different. When the SNR increases, the impact of I/Q imbalance on the FR is more critical resulting in more errors in the estimation than in the case without I/Q imbalance. For example, the FR increases nearly 9% at SNR = 8 dB. In the presence of I/Q imbalance, the FR still appears even when the SNR reaches 20 dB, while there is almost no errors in the positioning estimation in the absence of I/Q imbalance when SNR $\geq$ 16 dB. In average, the gain and phase imbalances of respectively 1.1 and 10° lead to the increase of about 5% errors in the positioning estimation.

Finally, we characterize the FGR due to the impact of I/Q imbalance. The SNR is set to 24 dB. Fig. 6 presents a contour plot of the FGR (in dB) for different values of gain and phase imbalances. It is clearly seen that the FGR increases when the values of I/Q imbalances become bigger, implying the positioning estimation errors also increase. This result suggests that the I/Q imbalance should be compensated for in the TRIPS system in order to ensure the correctness of the positioning estimation. The I/Q imbalance estimation and compensation can be integrated into the online channel estimation phase, using the fact that the training sequence is known beforehand. A lot of studies on I/Q imbalance compensation have been reported in the literature, i.e., [4], [10], however, the optimum I/Q imbalance compensation algorithm for TRIPS in terms of the complexity and its effectiveness is left for future study.

VI. Conclusion

We have studied the impact of I/Q imbalance in the time-reversal based indoor positioning systems (TRIPS). It has been analytically shown that the localization metric reduces in the presence of I/Q imbalance. As a consequence, the spatial focusing effect of the TRIPS also reduces whereas the error in the positioning estimation increases compared to the case of no I/Q imbalance. By numerical simulations, the reduction of focusing gain is about 0.5 dB and the average positioning estimation error is about 5% subject to the gain and phase imbalances of 1.1 and 10°, respectively, in the specified scenario. The focusing gain reduction and estimation error become more critical when the I/Q imbalance increases. The I/Q imbalance compensation is hence required in the TRIPS in order to achieve the correctness of the positioning estimation.

Acknowledgment

The authors would like to thank the financial supports of the Copine-IoT Innoviris project, the Icity.Brussels project and the FEDER/EFRO grant.

References

[1] Z. Yang, Z. Zhou, and Y. Liu, "From RSSI to CSI: Indoor localization via channel response," ACM Computing Surveys (CSUR), vol. 46, no. 2, article #25, Nov. 2013.

[2] J. Xiao, K. S. Wu, Y. Yi, and L. M. Ni, "FIFS: Fine-grained indoor fingerprinting system," 21st Int. Conf. on Computer Commun. and Netw. (ICCCN), pp. 1–7, Jul. 2012.

[3] Z.-H. Wu, Y. Han, Y. Chen, and K. J. R. Liu, "A time-reversal paradigm for indoor positioning system," IEEE Trans. Veh. Technol., vol. 64, no. 4, pp. 1331–1339, Apr. 2015.

[4] F. Horlin, A. Bourdoux, and L. Van der Perre, "Low-complexity EM-based joint acquisition of the carrier frequency offset and IQ imbalance," IEEE Trans. Wireless Commun., vol. 7, no. 6, pp. 2212–2220, Jun. 2008.

[5] F. Horlin, and A. Bourdoux, "Digital compensation for analog front-ends: A new approach to wireless transceiver design," John Wiley&Sons publisher, 1st edition, 2008.

[6] C. Chen, Y. Han, Y. Chen, and K. J. R. Liu, "Indoor global positioning system with centimeter accuracy using Wi-Fi," IEEE Signal Processing Magazine, vol. 33, no. 6, pp. 128–134, Nov. 2016.

[7] J. Vieira, E. Leitinger, M. Sarajlic, X. Li, and F. Tufvesson, "Deep convolutional neural networks for massive MIMO fingerprint-based positioning," IEEE 28th Annual Symposium on Personal, Indoor, and Mobile Radio Communications (PIMRC), pp. 1–6, Oct. 2017.

[8] Z. Yun, and M. F. Iskander, "Ray tracing for radio propagation modeling: Principles and applications," IEEE Access, vol. 3, pp. 1089–1100, Jul. 2015.

[9] G. Strang, "Linear algebra and its applications," Brook Cole publisher, 4th edition, 2006.

[10] Y.-H.. Chung, and S.-M. Phoong, "Channel estimation in the presence of transmitter and receiver I/Q mismatches for OFDM systems," IEEE Trans. Wireless Commun., vol. 8, no. 9, pp. 4476–4479, Sep. 2009.